Effects of Ion Group Content and Polyol Molecular Weight on Physical Properties of HTPB-based Waterborne Poly(urethane-urea)s

Shih Min Huang, Teng Ko Chen

Department of Chemical and Material Engineering, National Central University, Chung-Li City, Taoyuan County 320, Taiwan, Republic of China

Received 5 May 2006; accepted 14 March 2007
DOI 10.1002/app.26512
Published online 11 June 2007 in Wiley InterScience (www.interscience.wiley.com).

ABSTRACT: A series of waterborne poly(urethane-urea)s, WPUUs, based on using nonpolar hydroxyl-terminated polybutadiene (HTPB) as the soft segment, were successfully synthesized in this article. The effects of the COOH group content and soft-segment molecular weight (Mn_s) on the dispersion, morphology, and physical properties were investigated. Variations of the particle size, viscosity, and zeta potential were first governed by the hydrophilicity of the polymer chain, and then by the swelling derived from water. Fourier transfer infrared spectroscopy (FTIR) and differential scanning calorimetry (DSC) indicated that the degree of phase separation decreased as the COOH group content increased or as Mn_s decreased. However, the hydrogen bonding between the soft and hard segments and the two-phase mixing could not occur in this nonpolar HTPB-based WPUU system, indicating that the hard segments tended to form smaller domains and to pack more loosely. It was attributed to the fact that the presence of bulky ionic salt groups destroyed the ordered arrangement of the hard segments. In this case, the increases of the interface area between the soft and hard phases resulted in that the present behaviors were similar to the phase mixing. In tensile properties, HTPB-based WPUUs exhibited higher tensile stress, elongation at break, and modulus as the COOH group content decreased or as Mn_s decreased. In thermal degradation, the introduction of HTPB polyol improved the thermal stability of WPUU. © 2007 Wiley Periodicals, Inc. J Appl Polym Sci 105: 3794–3801, 2007

Key words: hydroxyl-terminated polybutadiene; waterborne poly(urethane-urea)s; dispersion; morphology; physical properties

INTRODUCTION

Waterborne poly(urethane-urea)s, WPUUs, are multiblock copolymers consisting of alternating the soft and hard segments. The ''soft segment'' typically is a polar polyol, such as polyether or polyester, with a glass transition temperature below ambient, which imparts elastomeric character to the polymer. The ''hard segment'' contains the highly polar urethane and urea linkages, typically with a glass transition above room temperature. Because of the hydrogen bonding, coulombic force and segmental polarity difference, these two segment types tend to phase-separate in the bulk.[1,2] The hard domains act as physical crosslinkers and reinforcing fillers. The variable physical properties of WPUUs depend strongly on the degree of phase separation and the cohesion of the hard domains. Besides, WPUUs not only conform to environmental emission legislation, but also reduce the consumptions of both cost and energy.[1] Therefore, they are widely used as the elastomer, coating, adhesive, and nanocomposite.[1–4]

The soft segments of polar polyol-based WPUUs have the ability to form the hydrogen bonding with the hard segments resulting in some degree of phase mixing. The partial phase mixing complicates the relationships between structure and properties.[1,5–7] Additionally, polar polyol-based WPUUs usually exhibit a higher absorption of water and a lower resistance to hydrolysis, reducing the range of applications. On the other hand, polyurethanes (PUs) made from nonpolar polyol, such as hydroxyl-terminated polybutadiene (HTPB) and polydimethylsiloxane, are generally thought to have almost complete phase separation and the higher resistance to hydrolysis. It is owing to the absence of the hydrogen bonding between the soft and hard segments. However, the reports of nonpoar polyol-based WPUUs are very few primarily owing to the fact that the prepolymers are too hydrophobic to disperse into an aqueous phase. In this study, we attempt to synthesize HTPB-based WPUUs containing several COOH group content and soft-segment molecular and to investigate the relationships between the morphology and physical properties.

Correspondence to: S. M. Huang (s8341002@cc.ncu.edu.tw).

Journal of Applied Polymer Science, Vol. 105, 3794–3801 (2007)

TABLE I
Formulations of HTPB-Based Waterborne Poly(urethane-urea)s

Sample	HTPB (mole)	H_{12}MDI (mole)	DMPA (mole)	EDA (mole)	TEA (mole)	Hard Segment Content (wt %)	COOH Content (wt %)
3400-55-1.2	0.132	1.588	0.266	1.188	0.266	55.0	1.2
3400-55-2.0	0.132	1.491	0.445	0.915	0.445	55.0	2.0
3400-55-2.5	0.132	1.431	0.555	0.743	0.555	55.0	2.5
3400-55-3.0	0.132	1.370	0.666	0.572	0.666	55.0	3.0
2050-55-1.2	0.220	1.604	0.266	1.118	0.266	55.0	1.2
2050-55-2.0	0.220	1.508	0.445	0.843	0.445	55.0	2.0
2050-55-2.5	0.220	1.447	0.555	0.672	0.555	55.0	2.5
2050-55-3.0	0.220	1.387	0.666	0.500	0.666	55.0	3.0
700-55-1.2	0.643	1.684	0.266	0.770	0.266	55.0	1.2
700-55-2.0	0.643	1.587	0.445	0.495	0.445	55.0	2.0
700-55-2.5	0.643	1.527	0.555	0.323	0.555	55.0	2.5
700-55-3.0	0.643	1.466	0.666	0.153	0.666	55.0	3.0

EXPERIMENTAL

Raw materials

The HTPB used in this study was characterized to have 96% *cis*-butadiene structure, and both molecular weight distribution and average hydroxyl functionality were equal to 2. The complete details for the synthesis and characterization of HTPB were given in our previous articles.[8,9] HTPB and dimethylolpropionic acid (DMPA; Lancaster) were dehydrated at 70°C in vacuum overnight before they were used. 4,4′-Dicyclohexylmethane diisocyanate (H12MDI; Bayer) and dibutyltin dilaurate (DBTDL; Aldrich) were used as received. Triethylamine (TEA; Tedia), ethylene diamine (EDA; Riedel-deHaen), 1-methyl-2-pyrrolidone (NMP; Tedia), dimethylacetamide (DMAc), and tetrahydrofuran (THF) were dehydrated by using 4 Å molecular sieves for 1 week before used.

Synthesis of WPUU dispersions

HTPB-based WPUU dispersions were synthesized by prepolymer mixing process.[1] A 500 mL four-necked round-bottom flask equipped with a mechanical stirrer, thermometer, nitrogen bubbler, and condenser was used as a reactor. HTPB (M_n = 700; 0.643 mol), DMPA (0.266 mol), DBTDL (1.0 wt % of H12MDI) and NMP (50 wt % of the total solid) were weighted out into the reactor, and then placed in a 80°C well-controlled oil bath for agitation. Subsequently, H12MDI (1.684 mol) was added dropwise into the flask and reacted at 80°C for about 4.5 h to obtain the NCO-terminated prepolymers. Changes in NCO value during the reaction were determined by a standard dibutylamine back-titration method.[10] Upon achieving the theoretical NCO value, the prepolymer solution was cooled down to 50°C. The NMP (50 wt % of the total solid) and TEA (0.266 mol) were added to adjust the viscosity and to neutralize at 50°C for 30 min, respectively. The 20°C water bath was used instead of the 50°C oil bath, and the water dispersion was carried out by adding the appropriate deionized water into the prepolymer solution to yield a solid content of 20 wt %. After the phase inversion was completed, the EDA (0.770 mol) was fed into the dispersion at 20°C. The polymer chain was extended at 50°C for the next 2 h. The sample was designated xxxx-yy-z.z, where the three terms were refer respectively, to HTPB molecular weight, hard-segment content (wt %) and the COOH group content (wt %). Accordingly, this composition was named 700-55-1.2 and the other formulations were presented in Table I. The COOH group content was defined as follows.[11]

$$\text{COOH group content (wt\%)} = \frac{\text{weight of COOH group in WPUU}}{\text{total weight of WPUU}} \times 100$$

Synthesis of model compound

A 250 mL four-necked round-bottom flask with a mechanical stirrer, thermometer, nitrogen bubbler and condenser was used as a reactor. Equal weights of DMAc and THF were mixed as the cosolvent. The 10 wt % solid content of the H12MDI (0.025 mol)/cosolvent solution was charged into the reactor and maintained at 0°C in an ice-water bath. EDA (0.025 mol)/cosolvent solution with 10 wt % solid content was added slowly into the reactor. After all of the EDA solution had been added, the chain extension was carried out for the next 2 h at room temperature, and the model compound obtained.

Film preparation

Films were prepared by casting the dispersion on a Teflon plate, followed by drying at 40°C for 4 days

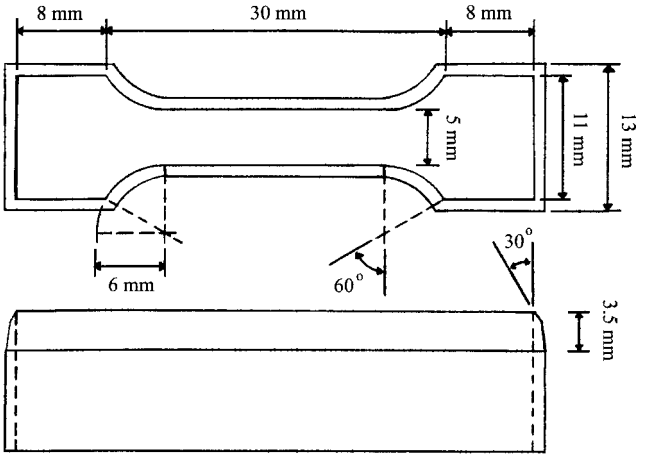

Scheme 1 The shape and dimension of die for tensile test.

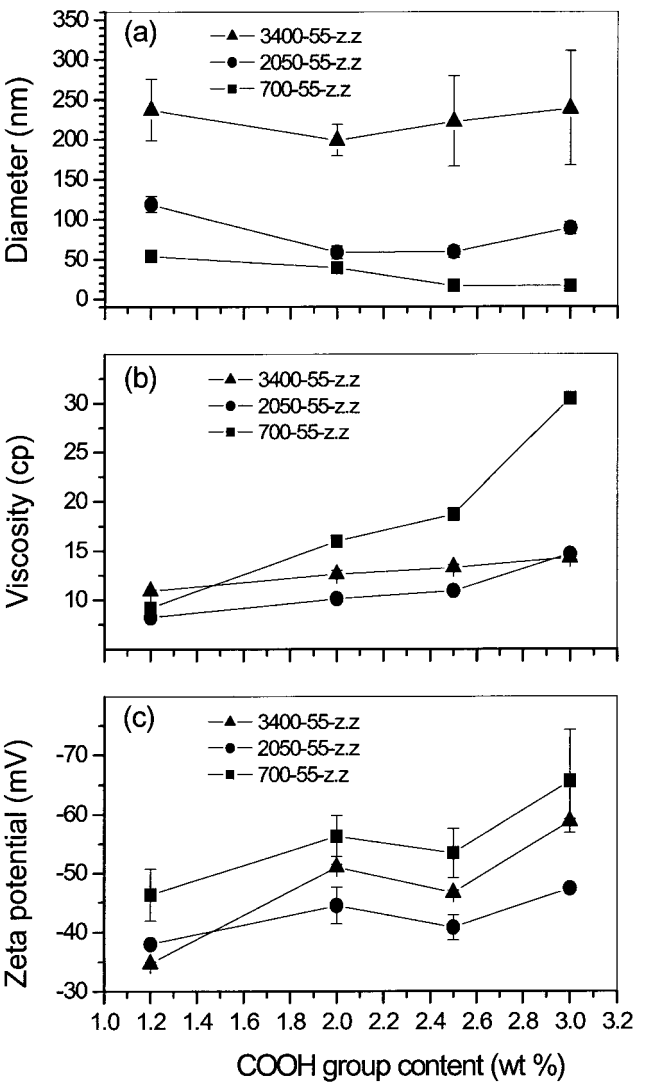

Figure 1 The (a) particle size, (b) viscosity and (c) zeta potential of dispersions were as a function of the COOH group content and HTPB molecular weight.

first, and then at 70°C for another 3 days. The complete dried films with about 0.2 mm thickness were obtained after they were placed in a vacuum oven at 70°C under 2–3 mmHg for 1 week. The model compound was dried by the same procedure.

Measurements

The diameter and zeta potential of dispersion particles were measured using an Autosizer-300 (Malvern) at 25°C. The dispersions were first diluted using deionized water to a solid content of 0.1 wt % and treated with ultrasonic waves before testing. The viscosity was determined using an LVDV-III cone-and-plate viscometer (Brookfield) at 25°C. Fourier-transfer infrared (FT-IR) spectra were collected using an FT/IR-410 spectrometer (Jasco) at a resolution of 2 cm^{-1} with 64 scans at room temperature. Differential scanning calorimetry (DSC) was performed using a Pyris-1 (Perkin–Elmer). Temperature calibration was performed by the melting points of cyclohexane and indium, while sapphire was utilized to calibrate the heat capacity. The sample with 10 ± 2 mg was initially quenched to −140°C, and

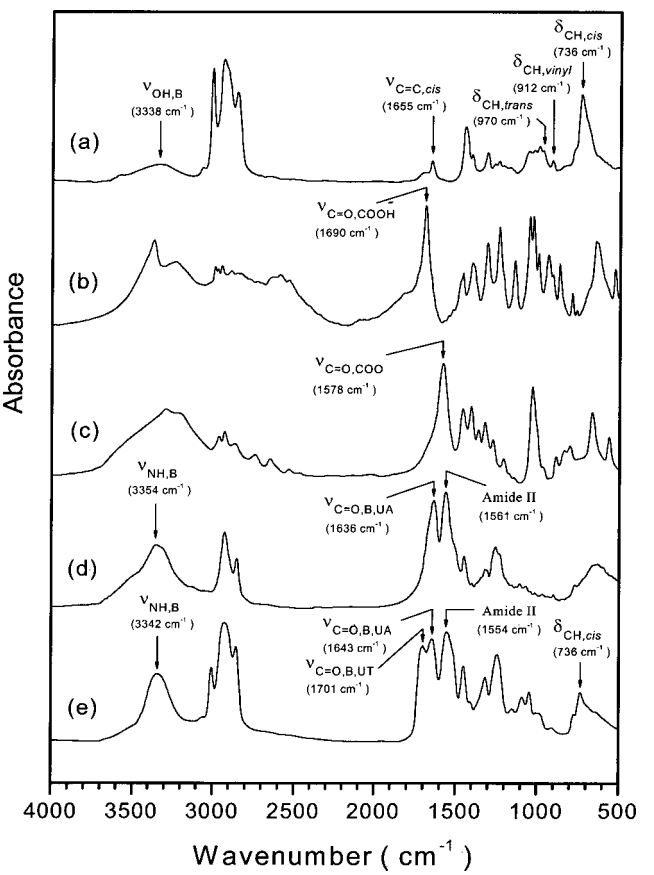

Figure 2 The FT-IR spectra of (a) HTPB, (b) DMPA, (c) NaOH-neutralized DMPA, (d) bisurea model compound and (e) 2050-55-2.0.

TABLE II
The Characteristic Absorptions of HTPB-Based WPUUs

	NH stretch		C=O stretch		
Sample	Free ($\nu_{NH,F}$)	Bonded ($\nu_{NH,B}$)	Bonded urethane ($\nu_{C=O,B,UT}$)	Bonded urea ($\nu_{C=O,B,UA}$)	Amide II
3400-55-1.2	–	3345	–	1639	1558
3400-55-2.0	–	3344	1699	1643	1556
3400-55-2.5	–	3342	1705	1651	1551
3400-55-3.0	–	3340	1705	1655	1549
2050-55-1.2	–	3344	1697	1641	1556
2050-55-2.0	–	3342	1701	1643	1554
2050-55-2.5	–	3342	1705	1651	1551
2050-55-3.0	–	3338	1705	1657	1547
700-55-1.2	3442	3331	1703	1645	1549
700-55-2.0	3441	3329	1703	1659	1537
700-55-2.5	3441	3331	1705	–	1531
700-55-3.0	3441	3329	1697	–	1529

then scanned to 180°C at a heating rate of 20°C/min with a helium purge. Tensile data were acquired from the averages of five tests at room temperature performed using an AG-I (Shimadzu). Specimens were stamped out using a particular dumbbell-shaped die, as presented in Scheme 1, and the cross-head speed was 30 mm/min. Thermogravimeteric analysis (TGA) was performed using a TGA-7 (Perkin–Elmer). The sample was first maintained at 50°C for 3 min to stabilize it, and then heated to 650°C at 10°C/min under a nitrogen purge.

RESULTS AND DISCUSSION

Dispersion properties

Figure 1 shows the effects of the COOH group content and HTPB molecular weight (Mn_s) on the particle size, viscosity and zeta potential of the WPUU dispersions. In Figure 1(a,b), the particle size and viscosity of the 700-55-z.z series decreases and increases, respectively, as the COOH group content increases. The former variation is attributable to an increase in segment hydrophilicity,[1] the latter is associated with an increase in the effective volume.[12] However, the particle sizes of the 2050-55-z.z and 3400-55-z.z series first decrease and then increase, but their viscosities still increase with increasing the COOH group content. Kim and Lee[6,7] once indicated that the electrical double-layer thickness and the effect of water swelling would be increased greatly when the COOH group content increased above a particular value. Hence, the further increase of the particle size is due to the increased extent in both factors. The extent of water swelling may correlate with the longer length of the hydrophilic hard segments. Additionally, the effective volume of the swollen particles increases, resulting in the continuous increase of the viscosity.

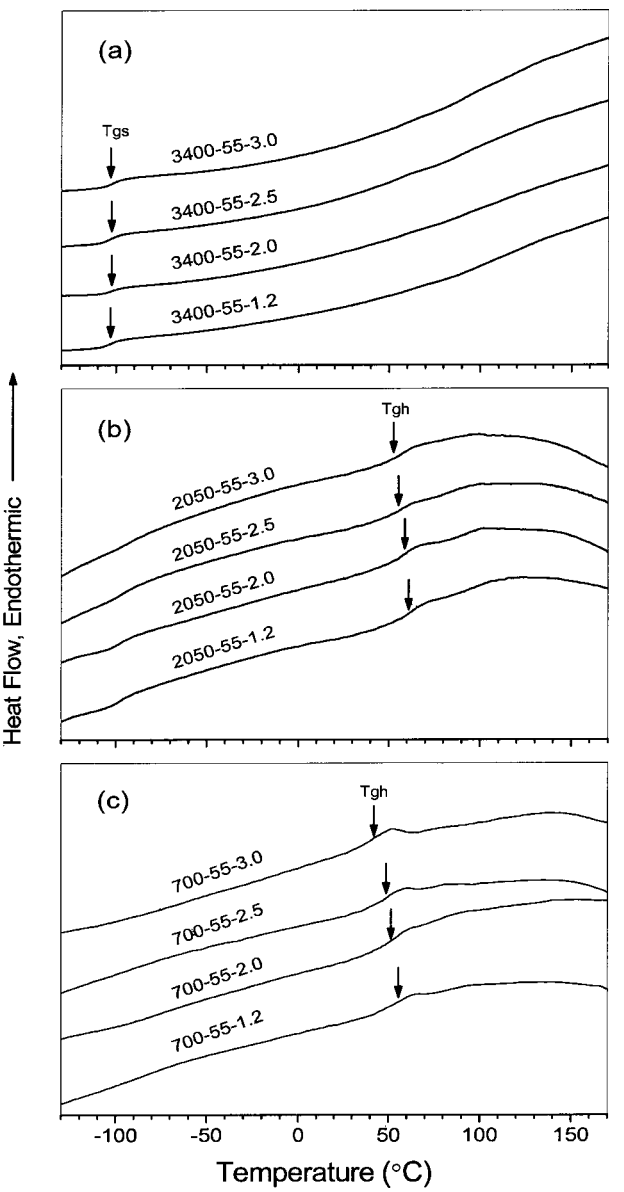

Figure 3 DSC thermograms of (a) 3400-55-z.z, (b) 2050-55-z.z and (c) 700-55-z.z series.

TABLE III
The Glass Transition Behaviors of HTPB Polyols and WPUU Samples

Samples	Glass transition data[a]					
	T_g (°C)	T_{gs} (°C)	ΔB (°C)	ΔB_s (°C)	ΔC_p (J/g °C)	ΔC_{p_s} (J/g °C)
HTPB-3400	−106		5		0.58	
3400-55-1.2		−103		7		0.33
3400-55-2.0		−101		8		0.33
3400-55-2.5		−101		9		0.32
3400-55-3.0		−100		9		0.31
HTPB-2050	−106		5		0.58	
2050-55-1.2		−99		9		0.30
2050-55-2.0		−99		9		0.30
2050-55-2.5		−97		11		0.25
2050-55-3.0		−97		12		0.21
HTPB-700	−105		5		0.57	
700-55-1.2		–		–		–
700-55-2.0		–		–		–
700-55-2.5		–		–		–
700-55-3.0		–		–		–

[a] T_{gs}, ΔB_s, and ΔC_{p_s} were defined as the glass transition temperature, the breadth of the glass transition, and heat capacity of the soft-segment.

In Figure 1(c), the zeta potentials of these three series exhibit a saw-toothed three-stage variation as the COOH group content increases. In the first stage, the increase of the zeta potential is corresponding to the increase of the salt group content because the electrostatic repulsion dominates the stability between the particles.[1] In the second stage, the zeta potential decreases. At this time, the PU chains have enough hydrophilicity and more easily disperse into the water phase to form smaller particles, which possess the sufficient stability[12] leading to the decreases in the necessity of electrostatic repulsion and the zeta potential. In the third stage, the zeta potential increases again, merely corresponding to the increase of the salt group content.

Fourier transfer infrared

Figure 2 shows several representative FT-IR spectra of monomer, model compound and WPUU. The characteristic absorptions of HTPB polyol[13] are labeled in Figure 2(a). In Figure 2(b,c), the considerable shift in the C=O stretching of DMPA from 1690 to 1578 cm^{-1} is caused by the complete transformation of the COOH group to the COO^- group. In Figure 2(d), the peaks of the H12MDI-EDA urea model compound at 3354, 1636, and 1561 cm^{-1} are assigned to the hydrogen-bonded (H-bonded) NH stretching ($\nu_{NH,B}$), H-bonded urea C=O stretching ($\nu_{C=O,B,UA}$)[14] and amide II band,[15] respectively. In Figure 2(e), the absorptions of HTPB-based WPUU at 3342, 1701, 1643, and 1554 cm^{-1} are identified individually as $\nu_{NH,B}$, H-bonded urethane C=O stretching ($\nu_{C=O,B,UT}$),[14] $\nu_{C=O,B,UA}$ and amide II band. Comparison of Figure 2(d,e), the $\nu_{NH,B}$ and amide II band of the urea model compound are at higher frequency than those of WPUU. These differences are attributed to the stronger hydrogen bonding and the close packing of the urea linkages than the urethane ones.

Bonart et al.[16] first proposed that one C=O group in the urea-based hard segment must be able to interact with at least two NH groups to form hydrogen bonds in different directions, as in ''three-dimensional (3D) hydrogen bonding.'' Subsequently, Wang and Cooper[17] found that $\nu_{NH,B}$ shifted to a higher frequency (from 3300 to 3320 cm^{-1}) and Sung et al.[18] observed that H-bonded C=O stretching shifted to a lower frequency (from 1660 to 1640 cm^{-1}) as the urea-linkage content increased. They all ascribed these results to the formation of 3D hydrogen bonding.

Table II lists the characteristic absorptions of HTPB-based WPUUs. In the 3400-55-z.z and 2050-55-z.z series, the $\nu_{NH,B}$ and amide II band shift to lower frequency, whereas the $\nu_{C=O,B,UT}$ and $\nu_{C=O,B,UA}$ move to higher frequency as the COOH group content increases. These results reveal that the hydrogen-bonding strength and the order in the hard-segment domains decrease, because of the bulky ionic salt groups provide the pronounced steric hindrance. Additionally, the effect of this steric hindrance will increase with decreasing Mn_s. The pronounced steric hindrance results in the appearance of the free NH stretching (at about 3441 cm^{-1}) in the 700-55-z.z series. Besides, the shifts of several absorptions of the 700-55-z.z series are simi-

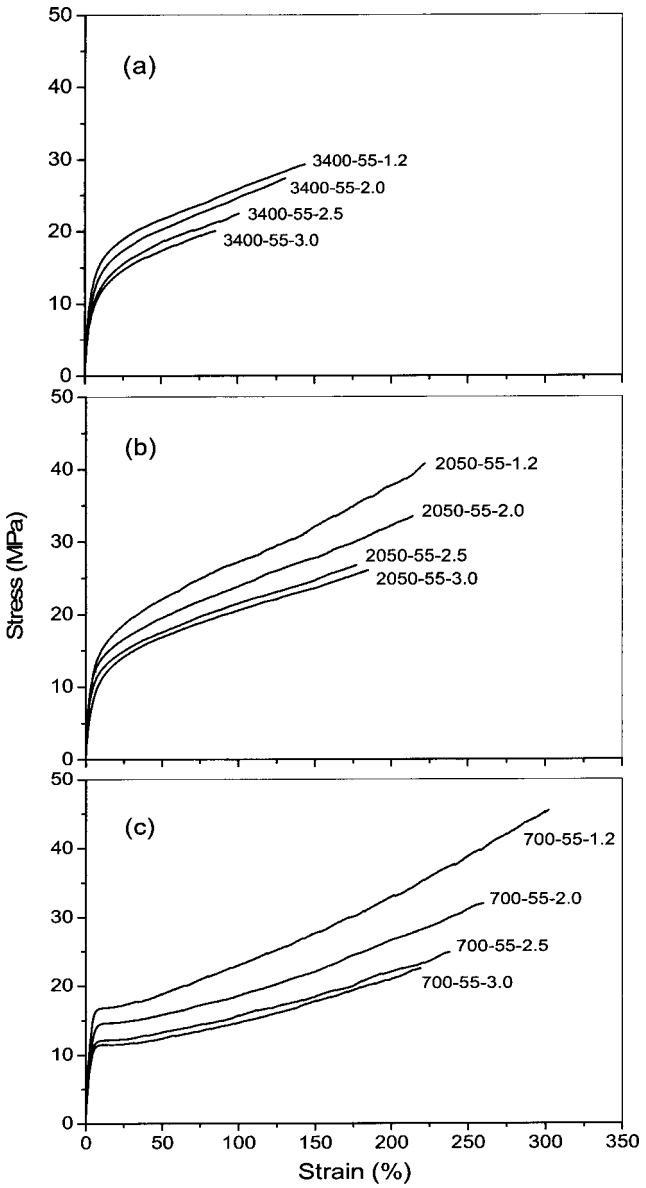

Figure 4 The stress-strain curves of (a) 3400-55-z.z, (b) 2050-55-z.z and (c) 700-55-z.z series.

lar to those of the other two series with increasing the COOH group content, except for the $\nu_{C=O,B,UT}$ of 700-55-3.0 at the lower frequency (1697 cm^{-1}). This $\nu_{C=O,B,UT}$ absorption is most probably influenced by the presence of a large amount of the free urea C=O stretching vibration (1695 cm^{-1}).[14]

The aforementioned results indicate that the degree of phase separation decreases as the COOH group content increases or Mn_s decreases. Note that no hydrogen bonding existed between the soft and hard segments of HTPB-based WPUU, which shall have much higher degree of phase separation.[14,19,20] Therefore, it reveals that the hard segments tend to form smaller domains and to pack more loosely in the soft phase. The increase of the interface area between the soft and hard phases results in that the present behaviors are similar to the phase mixing.

Differential scanning calorimetry

Figure 3 presents DSC thermograms of HTPB-based WPUUs. The magnitude of the glass transition behavior of the soft phase gradually decreases as Mn_s decreases, and no distinct transition can be observed in the 700-55-z.z series. The glass transition data of the soft segments and of HTPB polyols are summarized in Table III. The glass transition temperature (T_gs) and heat capacity (ΔC_{p_s}) of the soft segments of WPUUs are respectively, higher and much smaller than those of HTPB polyols. Similar results have been reported in many PU articles.[21–23] Since the chain ends of the soft segments were locked at the rigid surfaces of the hard phases (chain-end restriction), resulting in the decrease in the mobility of the soft segment and the increase of T_gs. The dispersed hard domains reduced the free volume of the soft segments (free-volume restriction), leading to the decrease of ΔC_{p_s}.[21–23]

TABLE IV
Tensile Properties of HTPB-Based WPUU Films

Sample	Tensile strength (MPa)	Elongation at break (%)	Modulus (MPa)		
			Young's	100%	200%
3400-55-1.2	30.8	144.2	203.8	25.8	–
3400-55-2.0	28.3	128.0	201.3	24.6	–
3400-55-2.5	20.9	90.3	158.1	22.4	–
3400-55-3.0	17.2	86.5	145.9	–	–
2050-55-1.2	34.9	199.3	207.7	27.2	37.7
2050-55-2.0	31.8	191.7	197.8	23.9	32.2
2050-55-2.5	27.3	157.9	171.5	21.5	–
2050-55-3.0	25.9	164.2	169.2	20.5	–
700-55-1.2	40.8	282.7	276.4	23.0	33.0
700-55-2.0	28.7	235.4	242.6	18.6	26.6
700-55-2.5	25.4	211.5	215.5	15.7	22.0
700-55-3.0	22.3	215.0	208.4	14.7	21.0

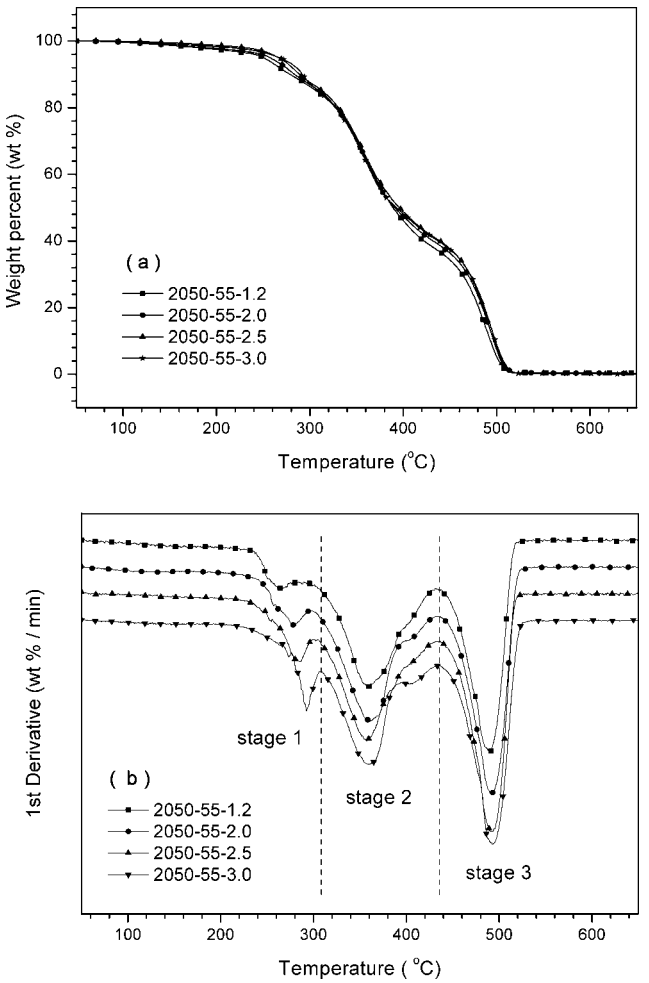

Figure 5 The (a) TGA and (b) DTGA curves of 2050-55-z.z series.

When Mn_s decreases or the COOH group content increases, the increase of T_{gs} and the decrease of ΔC_{p_s} indicate that the degree of phase mixing and free-volume restriction increase, respectively.[21–24] It shall be mentioned that the nonpolar HTPB-based WPUUs have a much higher degree of phase separation. Therefore, it demonstrates again that the hard segments prefer to form smaller domains and to pack more loosely because of the introduction of a large number of bulky ionic salt groups. On the other hand, in the 700-55-z.z series, T_{gs} is absent, but glass transition temperature of the hard segment ($T_{g,h}$) is present and close to that of the 2050-55-z.z series (Fig. 3). This fact reveals that the disappearance of T_{gs} in the 700-55-z.z series is independent of the phase mixing. It is most probably because of that the shorter soft segments encounter more considerable chain-end and free-volume restrictions from the dispersed hard domains.

Tensile properties

Figure 4 shows the stress-strain curves of the HTPB-based WPUU films, and the tensile data are summarized in Table IV. The tensile strength, the elongation at break and Young's modulus increase with decreasing Mn_s. It is well known that the hard domains act as the physical crosslinks, while WPUUs are made from shorter soft segments having smaller hard domains. At the same hard segment content, the smaller hard domains not only increase the crosslinking density leading to the increases in the tensile strength and Young's modulus, but also effectively prevent the cracks rapidly extended in the soft phases resulting in the increase of the elongation at break.[19,20,23] On the other hand, the tensile strength, the elongation at break and Young's modulus decrease as the COOH group content increases. It is ascribed to that the introduction of a large amount of the bulky ionic groups destroys the

TABLE V
The Onset Temperature and Weight Loss of HTPB-Based WPUUs

	Stage 1		Stage 2		Stage 3		wt % of formulation	
Sample	$T_{onset,1}$[a] (°C)	$W_{loss,1}$[b] (%)	$T_{onset,2}$ (°C)	$W_{loss,2}$ (%)	$T_{onset,3}$ (°C)	$W_{loss,3}$ (%)	TEA + DMPA	EDA + H12MDI
3400-55-1.2	253	15.1	335	46.4	470	38.3	6.26	48.74
3400-55-2.0	254	15.5	334	43.6	469	40.7	10.45	44.55
3400-55-2.5	259	15.9	336	42.3	471	41.3	13.05	41.95
3400-55-3.0	259	18.0	336	42.6	470	39.4	15.66	39.34
2050-55-1.2	246	12.2	334	50.0	466	37.5	6.26	48.74
2050-55-2.0	253	12.5	331	47.5	470	39.6	10.45	44.55
2050-55-2.5	259	12.8	332	46.7	470	40.4	13.05	41.95
2050-55-3.0	264	14.4	334	44.6	471	40.9	15.66	39.34
700-55-1.2	241	8.5	331	61.6	466	29.6	6.26	48.74
700-55-2.0	253	10.3	334	59.3	467	30.2	10.45	44.55
700-55-2.5	269	10.9	333	57.2	472	31.7	13.05	41.95
700-55-3.0	269	11.0	334	55.7	468	33.3	15.66	39.34

[a] Onset temperature of degradation.
[b] Percentage of weight loss.

ordered arrangement of the hard segments and let the hard domains act as ineffective crosslinkers.

Thermal degradation

Because of the pyrolysis behaviors of all three series are similar. The TGA and its differential (DTGA) curves of the 2050-55-z.z series are used respectively, as an example, and illustrated in Figure 5(a,b). It can be observed that HTPB-based WPUUs display a three-stage degradation. The onset temperature (T_{onset}) and weight loss (W_{loss}) in each stage are summarized in Table V. The amount of weight loss in first stage roughly corresponds to the formulation content of TEA and DMPA, revealing that the degradation probably begins from the liberation of TEA and the breakage of the urethane bond.[25] In the second stage, the amount of weight loss is closer to the sum of H12MDI and EDA indicating the dissociation of the urea bond.[26,27] Finally, the third-stage loss relates to the decomposition of HTPB.[28]

It is well-documented that the PUs have a lower thermal stability than the poly(urethane-urea)s, because the hydrogen bonding between urethane linkages is weaker than urea linkages.[27] Accordingly, the onset temperature of the first stage (Tonset,1) is reasonably expected to decrease as the COOH group content increases. However, Table V reveals an opposing tendency. This result may be associated with the rearrangement of ionic urethane linkages, such as ionic aggregation,[1,2,11,24] which retards the degradation of the first step. Subsequently, the onset temperatures of the second and third stages have no obvious changes with increasing the COOH group content. Comparison of polar polyol-based WPUUs (Tonset,1 at about 220°C),[26,27,29] the introduction of HTPB polyol improves the overall thermal stability of WPUUs.[28]

CONCLUSIONS

A series of HTPB-based WPUU dispersions had been successfully synthesized. In dispersion properties, the hydrophilicity of the polymer chain and the swelling derived from water dominate the variations in the particle size, viscosity and zeta potential.

The results of FT-IR and DSC were corresponding and indicated that the degree of phase separation decreased with increasing the COOH group content or with decreasing Mn_s. However, the HTPB-based WPUUs had a much higher degree of phase separation owing to no hydrogen bonding between the soft and hard segments. Hence, it implied that the hard segments tended to form smaller domains and to pack more loosely because of the introduction of bulky ionic salt groups providing the pronounced steric hindrance.

The tensile properties depended on the crosslinking density and effective crosslinkers. The DTGA curves exhibited the three-step degradation of HTPB-based WPUU films. The incorporation of HTPB polyol into the WPUU backbone improved the overall thermal stability.

References

1. Deterich, D. Prog Org Coat 1981, 9, 281.
2. Yen, M. S.; Kuo, S. C. J Appl Polym Sci 1998, 67, 1301.
3. Wen, T. C.; Wu, M. S.; Yang, C. H. Macromolecules 1999, 32, 2712.
4. Kim, B. K.; Seo, J. W.; Jeong, H. M. Eur Polym J 2003, 39, 85.
5. Hourston, D. J.; Williams, G.; Satguru, R.; Padget, J. D.; Pears, D. J Appl Polym Sci 1997, 66, 2035.
6. Kim, B. K.; Lee, Y. M. J Appl Polym Sci 1994, 54, 1809.
7. Kim, B. K.; Lee, J. C. J Polym Sci Part A: Polym Chem 1996, 34, 1095.
8. Chen, T. K.; Hwung, C. T. Proceedings of the 10th ROC Polymer Symposium; 1987.
9. Shieh, T. S.; Chui, J. Y.; Chen, T. K. Macromolecules 1998, 31, 1312.
10. Hepburn, C. Polyurethane Elastomers; Applied Science Publishers: New York, 1982.
11. Chen, Y.; Chen, Y. L. J Appl Polym Sci 1992, 46, 435.
12. Lovell, P. A.; El-Aasser, M. S. Emulsion Polymerization and Emulsion Polymers; Wiley: New York, 1997.
13. Silverstein, R. M.; Webster, F. X. Spectrometric Identification of Organic Compounds, 6th ed.; Wiley: New York, 1997; Chapter 3.
14. Born, L.; Hespe, H. Colloid Polym Sci 1985, 263, 335.
15. Skrovanek, D. J.; Howe, S. E.; Painter, P. C.; Coleman, M. M. Macromolecules 1985, 18, 1676.
16. Bonart, R.; Morbitzer, L.; Müller, E. H. J Macromol Sci Phys 1974, 9, 447.
17. Wang, C. B.; Cooper, S. L. Macromolecules 1983, 16, 775.
18. Sung, C. S. P.; Smith, T. W.; Sung, N. H. Macromolecules 1980, 13, 117.
19. Speckhard, T. A.; Cooper, S. L. Rubber Chem Technol 1986, 59, 405.
20. Smith, T. L. Polym Eng Sci 1977, 17, 129.
21. Seefried, C. G., Jr.; Koleske, J. V.; Critchfield, F. E. J Appl Polym Sci 975, 19, 2503.
22. Zdrahala, R. J.; Hager, S. L.; Gerkin, R. M.; Critchfield, F. E. J Elast Plast 1980, 12, 225.
23. Speckhard, T. A.; Gibson, P. E.; Cooper, S. L.; Chang, V. S. C.; Kennedny, J. P. Polymer 1985, 26, 55.
24. Yang, C. Z.; Grasel, T. G.; Bell, J. L.; Register, R. A.; Cooper, S. L. J Polym Sci Part B: Polym Phys 1991, 29, 581.
25. Chan, W. C.; Chen, S. A. Polymer 1988, 29, 1995.
26. Coutinho, F. M. B.; Delpech, M. C. Polym Degrad Stab 2000, 70, 49.
27. Matuszak, M. L.; Frisch, K. C. J Polym Sci Polym Chem Ed 1973, 11, 637.
28. Coutinho, F. M. B.; Delpech, M. C.; Alves, L. S. J Appl Polym Sci 2001, 80, 566.
29. Grassie, N.; Zulfiqar, M.; Guy, M. I. J Polym Sci Polym Chem Ed 1980, 18, 265.